SIAM J. APPL. MATH.
Vol. 74, No. 5, pp. 1418–1441

STABILITY AND SENSITIVITY ANALYSIS OF THE iSIR MODEL FOR INDIRECTLY TRANSMITTED INFECTIOUS DISEASES WITH IMMUNOLOGICAL THRESHOLD*

JUDE D. KONG†, WILLIAM DAVIS†, XIONG LI‡, AND HAO WANG§

Abstract. Most pathogenic diseases remain epidemic and endemic in the world, causing thousands of deaths annually in less developed countries. Yet, their dynamics are still not fully understood. In this paper, we carry out a thorough stability and sensitivity analysis of an iSIR which incorporates an infection term that explicitly includes a minimum infection dose (MID), and determine an invariant domain. We discover that if the MID (denoted c) is less than the bacterial carrying capacity K, we may have two steady states: the endemic or epidemic steady state, and the disease-free and bacteria-free steady state. The latter is unstable and the former is globally stable under a certain condition. On the other hand, if $c \geq K$, then up to four steady states may exist: an unstable endemic steady state, a locally stable endemic steady state, a conditionally globally stable disease-free steady state, and an unstable disease-free and bacteria-free steady state. We find that to control the period and intensity of the outbreaks, it might be better to focus on the bacterial carrying capacity rather than on the shedding rates.

Key words. indirect transmission, immunological threshold, infectious diseases, shedding, global stability analysis, sensitivity analysis

AMS subject classifications. 34Dxx, 34Cxx, 92B05

DOI. 10.1137/140959638

1. Introduction.

Infectious diseases are diseases caused by pathogenic microorganisms such as bacteria, viruses, parasites, and fungi. They can be spread either directly or indirectly. Direct transmission occurs when there is physical contact between an infected and a susceptible person. Examples of infectious diseases transmitted directly include common cold, scabies, and sexually transmitted diseases. Indirect transmission on the other hand, occurs when a susceptible individual comes into contact with a contaminated reservoir. Such diseases can be viral in nature, like rotavirus disease or hantavirus pulmonary syndrome [14, 29]; bacterial, such as cholera or legionellosis [1]; or parasitic, such as schistosomiasis, cryptosporidiosis or giardiasis [6, 12, 16]. The study of diseases spreading through human populations has received attention from mathematicians since the seminal papers of Kermack and McKendrick in the 1920s [31]. However, such attention has mostly been confined to diseases which spread directly. Among the few existing models for indirectly transmitted pathogenic diseases, the main ones that make use of ordinary differential equations are those built upon the Cappasso and Paveri-Fontana model [30] and the

*Received by the editors March 5, 2014; accepted for publication (in revised form) July 28, 2014; published electronically September 16, 2014.
http://www.siam.org/journals/siap/74-5/95963.html
†Department of Mathematical and Statistical Sciences, University of Alberta, Edmonton, AB, T6G 2R3 (jdkong@ualberta.ca, wdavis@math.ualberta.ca). The first author's work was supported by NSERC Discovery Grant RES0001528 and the FacSci Startup Fund RES0000381.
‡Laboratory of Mathematics and Complex Systems, School of Mathematical Sciences, Beijing Normal University, Ministry of Education, Beijing 100875, People's Republic of China (xli@bnu.edu.cn). This author's work was supported by NSFC 11031002 and the Fundamental Research Funds for the Central Universities.
§Corresponding author. Department of Mathematical and Statistical Sciences, University of Alberta, Edmonton, AB, T6G 2R3 (hao8@ualberta.ca). This author's work was supported by NSERC Discovery Grant RES0001528 and the FacSci Startup Fund RES0000381.

Codeço model [2]. While the Capasso and Paveri-Fontana model [30] consisted of two equations, with one for the infected compartment and the other for the aquatic pathogen community, Codeço included the susceptible population and the recovered population in the model as well. Denote S, I, and R as the susceptible, infected, and recovered compartments from standard SIR models. The recovered compartment is not stated explicitly, as the population is assumed to be of constant size and so the dynamics of the recovered compartment follow directly from the rest of the system noting that $H = S + I + R$, where H is the total population. The model is written

$$\begin{aligned}\dot{S} &= n(H - S) - a\lambda(B)S,\\ \dot{I} &= a\lambda(B)S - rI,\\ \dot{B} &= B(n_b - m_b) + eI.\end{aligned}$$

The birth and death rate are the same and denoted n. The parameter r represents recovery rate, and includes natural recovery and death. The pathogens have a net growth rate of proliferation n_b minus mortality m_b, and human contamination increases pathogen levels at a rate e proportional to the size of the infected class. The infective term consists of the maximum rate of exposure to contaminated water, a, multiplied by $\lambda(B) = \frac{B}{K+B}$ which is a Holling-II response curve. The use of such a term would overestimate the infectivity of low levels of pathogens, contrary to the idea of a minimum infectious dose, which we think is important.

Key features of the model are that the aquatic reservoir is represented very simply with a linear growth term and linear shedding contribution. This was because the ecological dynamics of the pathogen were not well understood at the time (they are still not completely understood), so Codeço started with the simplest way to model the pathogen population. Unless net growth is naturally zero ($n_b = m_b$), the bacterial population will die out exponentially in the absence of human shedding if $n_b < m_B$, or tend to infinity if $n_b > m_b$.

Hartley, Morris, and Smith [3] incorporated a hyperinfectious route of transmission to the Codeço model and Joh et al. [25], Tian and Wang [9], Jensen et al. [13], and Mukandavire et al. [32] have further built on and branched off from these models.

Joh et al.'s [25] model differs from the other models in that it takes into account the fact that pathogens have to enter the human body in higher concentrations to overwhelm the natural immune response [10] by incorporating a minimum infection dose (MID) into the incidence term. This MID is the rescaled value of the number of pathogens required to override the body's immune response. The infection term is a piecewise continuous function which is zero below the minimum infectious dose and a Holling-II response curve above this threshold. Joh et al. analyzed the stability of this model, but could not carry out all the essential stability and sensitivity analyses. In this paper we carry out a thorough stability and sensitivity analysis on the Joh et al. model. We show that if the bacterial population (B) is less than or equal to the ratio of the MID (denoted c) to the bacterial carrying capacity K, then we can only have an unstable disease-free and bacteria-free steady state; whereas if $B > c/K$ and $c < K$ we could have an unstable disease-free and bacteria-free equilibrium and a conditionally globally stable endemic or epidemic steady state. Else if $B > c/K$ and $c \geq K$ then we may have up to four steady states: an unstable endemic steady state, a locally stable endemic steady state, a conditionally globally stable disease-free steady state, and an unstable disease-free and bacteria-free steady state. Furthermore, we will show using sensitivity analysis that to control the frequency of the outbreaks and

the number of person that might be infected, it will be nice to focus on bacterial carrying capacity rather than on the shedding rate.

2. iSIR model formulation. One of the key differences of the iSIR model, proposed in Joh et al. [25], compared to standard SIR models is the incidence term. The rough idea is that humans consume bacteria constantly but do not always get sick. Unlike with viruses where only a small amount of exposure is required, for certain types of bacteria a significant amount of bacterial cells need to be ingested in order to override the body's immune response [10]. This threshold has been measured by the likes of Cash et al. [22] and others [7, 15, 23] to be at least 10^4 cells. Simply using Holling-I (or mass action) infection terms or Holling-II terms overestimates the infectivity of low levels of bacteria, since the standard Holling-I and Holling-II functions assume people will be infected with infinitesimally small densities of aquatic pathogens.

The incidence term used in this paper is $\alpha(B)S$, where $\alpha(B)$ is the pathogen density dependent component, and the S term is present for the same reasons as with standard SIR models. The indirect part of the incidence term is defined as

$$\alpha(B) = \begin{cases} 0, & B < c, \\ \frac{a(B-c)}{(B-c)+H}, & B \geq c. \end{cases}$$

When the pathogen density is below a rescaled level corresponding to the MID, there will be no infections even with a nonzero amount of susceptibles, and after the bacterial density is above that threshold, infections will occur via a Holling-II response, as shown in Figure 1.

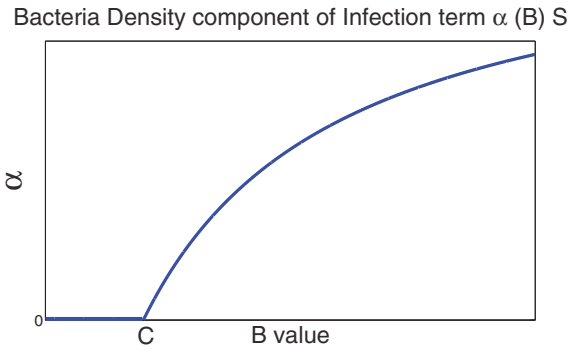

FIG. 1. *If bacterial levels are beneath the threshold c, $\alpha(B)$ is zero (no infections). If bacterial levels are above c, then $\alpha(B)$ is a Holling-II curve.*

As pathogens exist naturally in the aquatic environment, the iSIR model uses logistic bacterial growth in the absence of any infected people, in contrast to most other models which have linear terms for the pathogen growth and death [2, 3, 8]. The latter leads to exponential decay in the absence of infectives, which is consistent as many of those models assume that the aquatic reservoir of pathogens is not relevant to the cause of outbreaks, and so only the short term dynamics of freshly shedded pathogens are considered. In nonendemic areas, where the pathogen does not naturally exist in the environment, the linear form of the pathogen growth makes more sense than logistic growth, as used by Mukandavire et al. [32] in a study on recent

outbreaks of cholera in Zimbabwe. However, most models are intended for endemic areas.

The iSIR model has a positive contribution to the bacterial level when there are sick people shedding pathogens back into the reservoir. This occurs biologically with infected individuals contaminating the water supply through their pathogen laden feces. The dynamics are summarized in Figure 2.

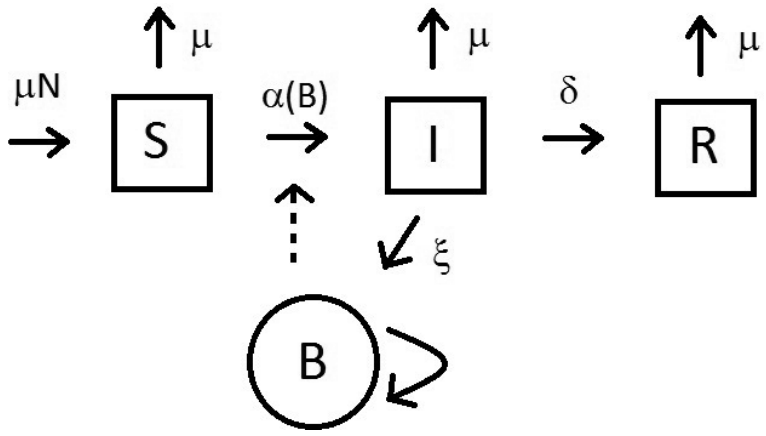

FIG. 2. *A flow diagram demonstrating the relationship between susceptibles (S), infectives (I), recovered (R), and pathogen (B). Humans have death rate μ, contribute to the pathogen reservoir at rate ξ, recover at rate δ, and are infected at rate $\alpha(B)$.*

The variables S, I, and R in Figure 2, are defined in the usual way as susceptible, infected, and recovered categories of the human population. The variable B represents the density of the pathogens in the aquatic reservoir. The first three equations sum to zero, thus the human population is of constant size. The equations for the model are as follows:

$$\frac{dS}{dt} = -\alpha(B)S - \mu S + \mu N, \tag{1a}$$

$$\frac{dI}{dt} = \alpha(B)S - \mu I - \delta I, \tag{1b}$$

$$\frac{dR}{dt} = \delta I - \mu R, \tag{1c}$$

$$\frac{dB}{dt} = rB\left(1 - \frac{B}{K}\right) + \xi I, \tag{1d}$$

$$N = S + I + R. \tag{1e}$$

This model was first proposed in Joh et al. [25], though the analysis was preliminary and here we will present a thorough examination of its dynamics. For numerical simulations, the values of the parameters described in Table 1 are taken from the literature. The large variations of the key parameter values for certain waterborne diseases are given in Table 2. Note that the ranges given in the second column of Table 2 are different from the pathogen shed rate ξ in Table 1. The pathogen shed rate is the number of pathogens shed by an infected per day divided by the total water volume of the reservoir (in liters).

TABLE 1
Model parameters.

Parameter	Description	Dimension
r	Maximum per capita pathogen growth efficiency	day^{-1}
K	Pathogen carrying capacity	cell liter^{-1}
H	Half-saturation pathogen density	cell liter^{-1}
a	Maximum rate of infection	day^{-1}
δ	Recovery rate	day^{-1}
ξ	Pathogen shed rate	cell liter^{-1} day^{-1}
μ	Per capita human birth/death rate	day^{-1}
N	Total population	persons
c	MID	cell liter^{-1}

TABLE 2
Key parameter values for certain waterborne diseases.

Disease	Number of pathogens shed by an infected/day (pathogen/day)	MID	Typical concentration (pathogen/liter)
Cholera	$10^{11} - 10^{12}$ [7]	$10^3 - 10^6$ [15, 27]	$10 - 10^3$ [21]
Cryptosporidiosis	10^8 [25]	$100 - 300$ [4]	$1 - 5$ [17]
Giardiasis	$10^8 - 10^9$ [24]	$10 - 100$ [24]	$1 - 5$ [17]
Rotavirus disease	$10^{12} - 10^{13}$ [20]	100 [25]	$10 - 1000$ [26]

3. Mathematical results. We can nondimensionalize the system as follows:

$$\mathbf{S} = \frac{S}{N}, \mathbf{I} = \frac{I}{N}, \mathbf{B} = \frac{B}{K},$$
$$\tau = \mu t, \mathbf{A} = \frac{a}{\mu}, \mathbf{C} = \frac{c}{K}, \mathbf{p} = \frac{\mu + \delta}{\mu}, \mathbf{q} = \frac{\xi N}{\mu K}, \mathcal{R} = \frac{r}{\mu}, \boldsymbol{\lambda} = \frac{H}{K}.$$

We redefine the per capita infection rate α accordingly as

$$\overline{\alpha}(\mathbf{B}) = \begin{cases} 0, & \mathbf{B} < \mathbf{C}, \\ \frac{\mathbf{A}(\mathbf{B}-\mathbf{C})}{(\mathbf{B}-\mathbf{C})+\boldsymbol{\lambda}}, & \mathbf{B} \geq \mathbf{C}. \end{cases}$$

The boldface is now dropped and we arrive at the following nondimensionalized iSIR system:

$$\frac{dS}{d\tau} = -\overline{\alpha}(B)S - S + 1, \tag{2a}$$
$$\frac{dI}{d\tau} = \overline{\alpha}(B)S - pI, \tag{2b}$$
$$\frac{dB}{d\tau} = \mathcal{R}B(1 - B) + qI. \tag{2c}$$

3.1. Forward invariance. First note that in dimensional terms, if $S = 0$, then $\dot{S} = N > 0$ and so $S(t) > 0$ for $t > 0$. If $I = 0$, then $\dot{I} = \overline{\alpha}(B)S$ and because $\overline{\alpha}(B) \geq 0$ by definition, then $I \geq 0$ as well. The third equation of (2.1) gives us that $\dot{R} = \delta I$ when $R = 0$, thus $R(t) \geq 0$. As $S + I + R = N$, we get that S, I, $R \leq N$ in the usual way. This transfers over to the nondimensional quantities of S, I, and R, the last of which we typically exclude. We have that $0 \leq S + I \leq 1$ in particular.

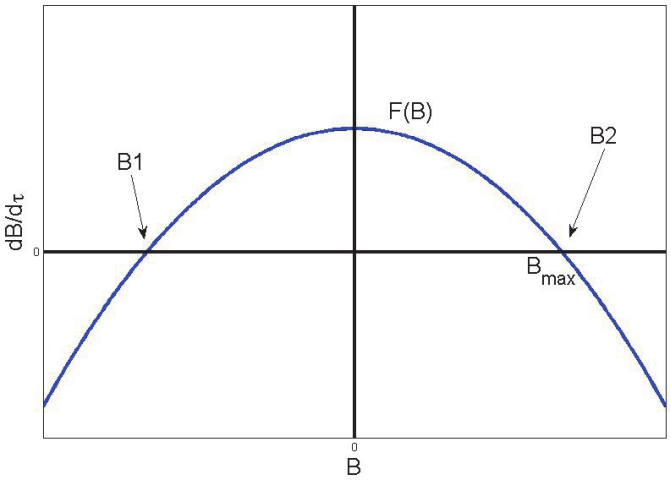

FIG. 3. *The derivative of the bacteria vs. bacterial population. When above B_{max}, the derivative becomes negative. When B is zero, the derivative is positive.*

Once again we drop the boldface for convenience. Looking at the third equation of the nondimensional system we can make note that $\mathcal{R}B(1-B)+qI \leq \mathcal{R}B(1-B)+q$ as $I \leq 1$. Define $F(B) := \mathcal{R}B(1-B)+q$ which has roots $B_{1,2} = \frac{\mathcal{R}\pm\sqrt{\mathcal{R}^2+4\mathcal{R}q}}{2\mathcal{R}}$ and note the smaller root $B_1 = \frac{\mathcal{R}-\sqrt{\mathcal{R}^2+4\mathcal{R}q}}{2\mathcal{R}} < 0$ because of the positivity of the parameters. The other root B_2 is clearly positive and is denoted as $B_{max} = \frac{\mathcal{R}+\sqrt{\mathcal{R}^2+4\mathcal{R}q}}{2\mathcal{R}} > 1$. The graph of $F(B)$ is pictured in Figure 3. When $B = 0$, we see that $\dot{B} = qI$ and thus $B(\tau) \geq 0$ for $\tau > 0$. If $B(0) \in [0, B_{max})$ then $B(\tau) \in [0, B_{max})$ for any $\tau > 0$. The invariant region is pictured in Figure 4 and we summarize with a proposition.

PROPOSITION 3.1 (feasible region). *The set*

$$\Omega = \{(S, I, B) : 0 < S + I \leq 1, 0 \leq B \leq B_{max}, S > 0 \text{ and } I \geq 0\}$$

defines a forward invariant region of system (3.1).

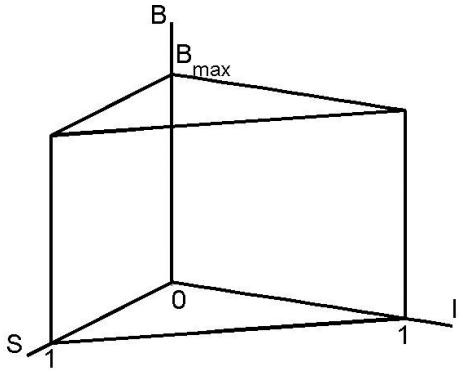

FIG. 4. *The forward invariant region of system* (3.1).

3.2. Equilibria of the system. Clearly $E_0 = (1, 0, 0)$ is a steady state of (3.1) and biologically it corresponds to a disease-free and bacteria-free population. When $C \geq 1$, i.e, when the in-reservior pathogen density is less than or equal to the rescaled MID, this means $\bar{\alpha}(1) = 0$ and $E_1 = (1, 0, 1)$ is an equilibrium corresponding to a disease-free state with bacteria at carrying capacity. When $C < 1$, i.e, when the in-reservior pathogen density is greater than the rescaled MID, we get that $\overline{\alpha}(1) \neq 0$ and so $E_1 = (1, 0, 1)$ is not an equilibrium and (3.1) has no equilibrium (S^*, I^*, B^*) with $B^* \leq C$ except E_0. The more complicated steady state $E^* = (S^*, I^*, B^*)$ arises when $B^* > C$ which causes $\overline{\alpha}(B^*) \neq 0$. Thus, system (3.1) implies that

$$S^* = \frac{B^* - C + \lambda}{(A+1)(B^* - C) + \lambda},$$
$$I^* = \frac{1}{p}\left(\frac{A(B^* - C)}{(A+1)(B^* - C) + \lambda}\right) = \frac{\mathcal{R}}{q} B^*(B^* - 1).$$

The expressions for I^* can be combined to form the equation

$$B^*(B^* - 1)\left(B^* - \left(C - \frac{\lambda}{A+1}\right)\right) = \frac{q}{p\mathcal{R}}\frac{A}{A+1}(B^* - C). \tag{3}$$

Define $F_1(B) = f(B) - g(B)$, where $f(B) = B(B-1)\big(B - C + \frac{\lambda}{A+1}\big)$ and $g(B) = \frac{q}{p\mathcal{R}}\frac{A}{A+1}(B - C)$. Denote $B_3 = C - \frac{\lambda}{A+1}$ so that if $C < 1$ we see that

$$F_1(B_3) = \frac{q}{p\mathcal{R}}\frac{A}{A+1}\frac{\lambda}{A+1} > 0,$$
$$F_1(C) = C(C-1)\left(\frac{\lambda}{A+1}\right) - 0 < 0.$$

Therefore there exists a root $\overline{B_1} \in (B_3, C)$. However, as $\overline{B_1} < C$ then $\bar{\alpha}(\overline{B_1}) = 0$ and (3) does not apply. We have that $f(0) = 0$ and $g(0) < 0 \implies f(0) > g(0) \implies F_1(0) = f(0) - g(0) > 0$. For $B = b \ll 0$ we have that $f(b) < 0$, $g(b) < 0$, and $f(b) < g(b) \implies F_1(b) = f(b) - g(b) < 0$. Since $F_1(0) > 0$ and $F_1(b) < 0$ for $b \ll 0$ and F_1 is continuous on $(0, b)$, using the Intermediate Value Theorem (IVT) we can find a $\bar{B}_2 \in (0, b)$ such that $F_1(\bar{B}_2) = 0$. Since $\bar{B}_2 < 0$, it is not in the feasible region for Ω. Lastly,

$$F_1(1) = -\frac{q}{p\mathcal{R}}\frac{A}{A+1}(1 - C) < 0,$$
$$F_1(B_{max}) = (B_{max} - C)\left[\frac{q}{\mathcal{R}} - \frac{q}{\mathcal{R}}\frac{1}{p}\frac{A}{A+1}\right] + \frac{q}{\mathcal{R}}\frac{\lambda}{A+1} > 0.$$

The latter is true as $p > 1, B_{max} > 1$, and thus we conclude that there exists $B^* \in (1, B_{max})$ when $C < 1$ and it is the unique positive solution to (3), giving us a unique interior equilibrium $E^* = (S^*, I^*, B^*)$.

Note that $\lim_{C \to 1^-} B^*(C) = 1$, as the x-intercept of $g(B)$ is 1 when $C \to 1^-$ and $f(1) = 0$. As C increases over the value 1, E^* becomes E_1 or vice versa if C is decreased.

We conclude that when $C \geq 1$, $f(B)$ and $g(B)$ are as in Figure 5 and there are $0, 1$, or 2 roots of (3) with bacterial values greater than the MID (C). For these values of $B^+_{1,2}$, we find S^+_i and I^+_i in the same way as with E^*, leading us to two distinct equilibria $E^+_{1,2}$.

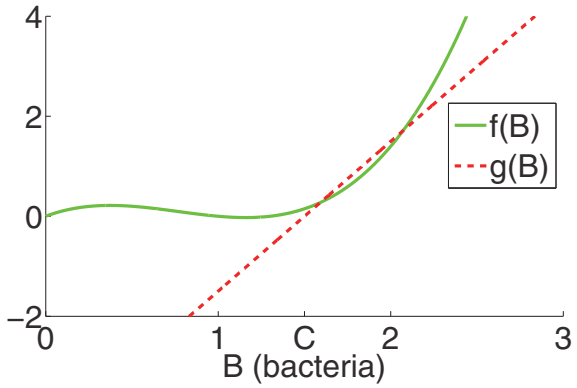

FIG. 5. *The left- and right-hand sides of* (3) *when* $C \geq 1$. *There can be* 0, 1, *or* 2 *intersections with bacterial values above the MID.*

As C is greater than 1, it is larger than all of the roots of $f(B)$. Thus, $f(B)$ is concave up on $[C, \infty)$ and $f'(B) \geq f'(C) > 0$ for $B \in [C, \infty)$. If the slope of $g(B)$ is less than $f'(C)$, there will be no endemic equilibria, as $g(B)$ will always be below $f(B)$ and there will be no intersections. Defining $\zeta = \frac{q}{p\mathcal{R}}$ and working backwards, we see that

$$\begin{aligned} & \zeta < f'(C) \\ \implies & \zeta \frac{A}{A+1} < f'(C) \\ \implies & g'(B) < f'(C), \end{aligned}$$

meaning that

$$\zeta < f'(C) \tag{4}$$

is a sufficient condition for there being no internal equilibria when $C \geq 1$. In dimensional parameters, $\zeta = \left(\frac{\xi N}{\mu+\delta}\right)\left(\frac{\mu}{rK}\right)$, and so ζ is proportional to the shedding rate ξ. This motivates the definition of the condition for no internal steady states, as we shall see later. We summarize with a proposition.

Remark 3.2 (biological interpretation of ζ). $\zeta = \left(\frac{\xi N}{\mu+\delta}\right)/\left(\frac{1}{\mu}(rK)\right)$ is the ratio of the average number of pathogens shed over the time course of infection if all individuals were infected to the average number of pathogens reproduced in the reservoir over the time course of an uninfected individual.

PROPOSITION 3.3 (existence of equilibria). *The equilibrium* $E_0 = (1, 0, 0)$ *always exists in* Ω.

- *When* $C < 1$ *(equivalently,* $c < K$*), i.e, when the in-reservior pathogen density is greater than the rescaled MID, there exist two equilibria,* E_0 *on* $\partial\Omega$ *and a unique endemic equilibrium* E^* *in* $\mathring{\Omega}$.
- *When* $C \geq 1$ *(equivalently,* $c \geq K$*), i.e, when the in-reservior pathogen density is less than or equal to the rescaled MID, then* $E_1 = (1, 0, 1)$ *is also an equilibrium and there can be up to two internal equilibria* $E^+_{1,2}$.
  - *If* $\zeta < f'(C)$, *there are no internal equilibria, and only* E_1 *and* E_0 *exist.*

3.3. Local stability of E_0, E_1, and E^*. We calculate the Jacobian to analyze the local stability of each of the equilibria. For the simpler case of $B \le C$,

$$J_1(S,I,B) = \begin{pmatrix} -1 & 0 & 0 \\ 0 & -p & 0 \\ 0 & q & R - 2\mathcal{R}B \end{pmatrix},$$

and for $B > C$,

$$J_2(S,I,B) = \begin{pmatrix} \frac{-A(B-C)}{(B-C)+\lambda} - 1 & 0 & \frac{-A\lambda}{[(B-C)+\lambda]^2}S \\ \frac{A(B-C)}{(B-C)+\lambda} & -p & \frac{A\lambda}{[(B-C)+\lambda]^2}S \\ 0 & q & \mathcal{R} - 2\mathcal{R}B \end{pmatrix}.$$

When $C \ge 1$, the equilibria are $E_0 = (1,0,0), E_1 = (1,0,1)$, and up to two $E_i^+ = (S_i^+, I_i^+, B_i^+)$. For $C \ge 1$, we use J_1 and find that E_0 has eigenvalues $-1, -p$, and $\mathcal{R}$, which indicates that E_0 is a saddle-point equilibrium, as all parameter values are assumed positive. E_1 in this case has eigenvalues $-1, -p$, and $-\mathcal{R}$ and thus we can conclude that when $C \ge 1$, the equilibrium $(1,0,1)$ is locally asymptotically stable, that is, the disease-free equilibrium is locally asymptotically stable. Also, for $C < 1$, E_0 is a saddle-point equilibrium for the same reasons.

Now considering E^* and using the nondimensionalized system (3.1), we obtain

$$S^* = \frac{B^* - C + \lambda}{(A+1)\left(B^* - C + \frac{\lambda}{A+1}\right)} = \frac{B^* - C + \lambda}{(A+1)\left(\frac{q}{p\mathcal{R}}\frac{A}{A+1}(B^* - C)\frac{1}{B^*(B^*-1)}\right)},$$

$$S^* = \frac{p\mathcal{R}}{Aq}\frac{B^*}{B^* - C}(B^* - 1)(B^* - C + \lambda).$$

We will use γ for eigenvalues as the traditional λ is already used elsewhere. We can compute

$$\begin{aligned} \det(\gamma I - J_{E^*}) &= \det \begin{pmatrix} \gamma + \frac{A(B^*-C)}{(B^*-C)+\lambda} + 1 & 0 & \frac{A\lambda}{[(B^*-C)+\lambda]^2}S^* \\ \frac{-A(B^*-C)}{(B^*-C)+\lambda} & \gamma + p & \frac{-A\lambda}{[(B^*-C)+\lambda]^2}S^* \\ 0 & -q & \gamma + \mathcal{R}(2B^* - 1) \end{pmatrix} \\ &= \left(\gamma + \frac{A(B^*-C)}{B^* - C + \lambda} + 1\right)\left[(\gamma + p)(\gamma + \mathcal{R}(2B^* - 1)) - \frac{A\lambda q}{(B^* - C + \lambda)^2}S^*\right] \\ &\quad + \frac{A^2\lambda q}{(B^* - C + \lambda)^3}(B^* - C)S^*. \end{aligned}$$

Define $F_2(\gamma) := \det(\gamma I - J_{E^*})$, $h := A\frac{B^*-C}{B^*-C+\lambda} + 1$, and $m := \frac{A\lambda q}{(B^*-C+\lambda)^2}S^*$. Later we will make use of the following alternate forms of these definitions:

$$h = A\left(\frac{B^* - C}{B^* - C + \lambda} + \frac{1}{A}\right) = \frac{(A+1)(B^* - C) + \lambda}{B* - C + \lambda} > 1$$

and

$$m = \frac{A\lambda q}{(B^* - C + \lambda)^2}\frac{p\mathcal{R}}{Aq}\frac{B^*}{B^* - C}(B^* - 1)(B^* - C + \lambda) = p\mathcal{R}\frac{\lambda}{B^* - C + \lambda}\frac{B^* - 1}{B^* - C}B^*.$$

We can rewrite the characteristic equation with these new expressions taken into account as follows:

$$\begin{aligned}F_2(\gamma) &= (\gamma+h)[(\gamma+p)(\gamma+\mathcal{R}(2B^*-1))-m]+\frac{A^2\lambda q}{(B^*-C+\lambda)^3}(B^*-C)S^*\\ &= (\gamma+h)[\gamma^2+(\mathcal{R}(2B^*-1)+p)\gamma+p\mathcal{R}(2B^*-1)-m]+\frac{A^2\lambda q}{(B^*-C+\lambda)^3}(B^*-C)S^*\\ &= \{\gamma^3+\mathcal{R}(2B^*-1+p)\gamma^2+[p\mathcal{R}(2B^*-1)-m]\gamma+h\gamma^2+h(\mathcal{R}(2B^*-1)+p)\gamma\\ &\quad +[p\mathcal{R}(2B^*-1)-m]h\}+\frac{A^2\lambda q}{(B^*-C+\lambda)^3}(B^*-C)S^*.\end{aligned}$$

The Routh–Hurwitz coefficients of the above expression are

$$\begin{aligned}b_3 &= 1,\\ b_2 &= \mathcal{R}(2B^*-1)+p+h,\\ b_1 &= p\mathcal{R}(2B^*-1)-b+h(\mathcal{R}(2B^*-1)+p),\\ b_0 &= [p\mathcal{R}(2B^*-1)-b]h+\frac{A^2\lambda q}{(B^*-C+\lambda)^3}(B^*-C)S^*,\end{aligned}$$

and note that the Routh–Hurwitz stability criterion requires

$$b_1,b_2,b_3>0 \quad \text{and} \quad b_2b_1>b_3b_0$$

as a sufficient condition for stability of the equilibrium. Clearly b_2 and b_3 are positive, and if $p\mathcal{R}(2B^*-1)-m>0$ then $b_1,b_0>0$. As $C<1$ for the internal equilibrium E^* to exist, $B^*-1<B^*-C$ so that $\frac{B^*-1}{B^*-C}<1$.
Thus

$$m=p\mathcal{R}\frac{\lambda}{B^*-C+\lambda}\frac{B^*-1}{B^*-C}B^*<p\mathcal{R}B^*$$

and so

$$p\mathcal{R}(2B^*-1)-m>p\mathcal{R}(2B^*-1)-p\mathcal{R}B^*=p\mathcal{R}(B^*-1)>0,$$

which means $b_1,b_0>0$.

As for the second condition $b_2b_1>b_3b_0$, we have the following expression

$$\begin{aligned}b_1b_2 &= [(h+p)\mathcal{R}(2B^*-1)+hp-m][\mathcal{R}(2B^*-1)+(p+h)]\\ &= (h+p)\mathcal{R}^2(2B^*-1)^2+(h+p)^2\mathcal{R}(2B^*-1)+(hp-m)\mathcal{R}(2B^*-1)\\ &\quad +(h+p)(hp-m).\end{aligned}$$

We can define

$$\begin{aligned}B_1 &= 2hp\mathcal{R}(2B^*-1)-hm,\\ B_2 &= p\mathcal{R}^2(2B^*-1)^2-m\mathcal{R}(2B^*-1),\\ B_3 &= p^2\mathcal{R}(2B^*-1)-pm,\\ B_4 &= h\mathcal{R}^2(2B^*-1)^2+h^2\mathcal{R}(2B^*-1)+h^2p+hp^2+hp\mathcal{R}(2B^*-1).\end{aligned}$$

Using the definition of S^*, we can express

$$\begin{aligned} b_3b_0 &= b_0 \\ &= [p\mathcal{R}(2B^*-1)-m]h + \frac{A^2\lambda q}{(B^*-C+\lambda)^3}(B^*-C)\frac{p\mathcal{R}}{Aq}\frac{B^*}{B^*-C}(B^*-1)(B^*-C+\lambda) \\ &= [p\mathcal{R}(2B^*-1)-m]h + A\lambda p\mathcal{R}\frac{B^*}{(B^*-C+\lambda)^2}(B^*-1). \end{aligned}$$

Now we check to see if the inequality $b_1b_2 > b_0$ is satisfied by noting that

$$\begin{aligned} &(B^*-C)(2B^*-1) > (B^*-1)B^* \\ \Rightarrow\ &\frac{B^*-C}{B^*-C+\lambda}(2B^*-1) + \frac{1}{A}(2B^*-1) > (B^*-1)\frac{B^*}{B^*-C+\lambda} \\ \Rightarrow\ &Ap\mathcal{R}\left(\frac{B^*-C}{B^*-C+\lambda}+\frac{1}{A}\right)(2B^*-1) > Ap\mathcal{R}(B^*-1)\frac{B^*}{B^*-C+\lambda} \\ \Rightarrow\ &hp\mathcal{R}(2B^*-1) > Ap\mathcal{R}\lambda(B^*-1)\frac{B^*}{(B^*-C+\lambda)^2} \\ \Rightarrow\ &2hp\mathcal{R}(2B^*-1)-hm > hp\mathcal{R}(2B^*-1) + Ap\mathcal{R}\lambda\frac{B^*}{(B^*-C+\lambda)^2}(B^*-1)-hm. \end{aligned}$$

The left-hand side of the above inequality is precisely B_1 and the right-hand side is b_0. Recall that $m < p\mathcal{R}B^*$, and so

$$p\mathcal{R}^2(2B^*-1)^2 - m\mathcal{R}(2B^*-C) > p\mathcal{R}^2(2B^*-1)^2 - p\mathcal{R}^2B^*(2B^*-1) > 0$$

and

$$p^2\mathcal{R}(2B^*-1) - pm > p^2\mathcal{R}(2B^*-1) - p^2\mathcal{R}B^* = p^2\mathcal{R}(B^*-1) > 0.$$

Thus $B_2, B_3 > 0$ and clearly $B_4 > 0$. Lastly,

$$b_1b_2 = \sum_1^4 B_i > B_1 > b_0.$$

Thus the Routh–Hurwitz conditions are satisfied and E^* is locally asymptotically stable.

3.4. Local stability of $E_{1,2}^+$. When E_i^+ exists, things are more complicated as we lack exact expressions for the equilibrium quantities, and so the local stability is difficult to find analytically. Numerically, it can be demonstrated that E_1^+ (with $B_1^+ < B_2^+$) is a saddle, and E_2^+ is attracting. For example, this can be seen with parameters $A = 1e3, C = 2, p = 10, q = 1e3, \mathcal{R} = 30$, and $\lambda = 1$,. With these parameters E_1^+ and E_2^+ both exist and are given as $E_1^+ = (0.3986, 0.0601, 2.0015)$ and $E_2^+ = (0.0036, 0.0996, 2.3898)$. The eigenvalues corresponding to these steady states are $\gamma_1 = (-0.9969, 580.8379, -682.4401)$, $\gamma_2 = (-292.1109, -10.6368, -102.1349)$.

The equilibria E_1 and E_2^+ are both locally stable and a situation of bistability occurs, as observed in Figure 6(a). Almost every solution approaches either the endemic equilibrium or the disease-free equilibrium, depending on initial conditions. Numerically we observe that the basin of attraction is much larger for the endemic equilibrium E_2^+, meaning that a greater range of initial conditions will lead to an

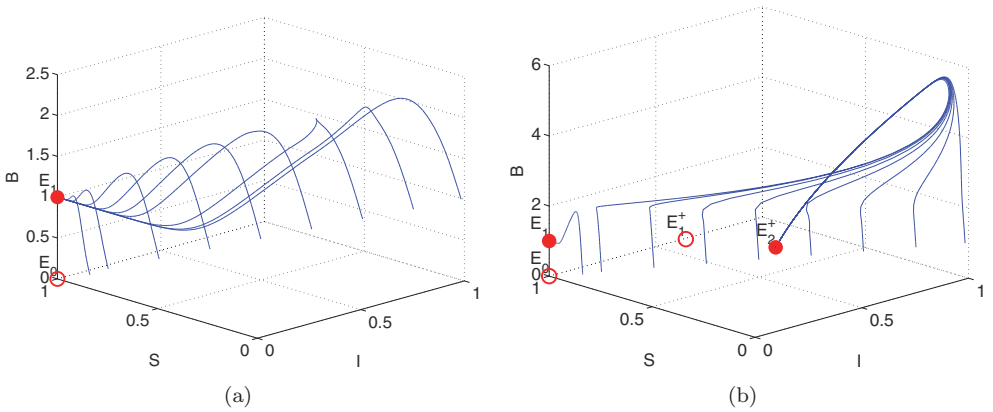

FIG. 6. *Trajectories in the phase space for $C > 1$ and $B^* \geq C$. Stable equilibria are marked as $\bullet$ while unstable equilibria are marked as $\circ$.* (a) *$\zeta < f'(C)$ ($\zeta = 0.5$, $f'(C) = 2.0297$). Only two equilibrium points exist: a saddle E_0 and an attracting equilibrium E_1, the number of infected persons goes to zero as $t \to \infty$. The values used for the parameters are as follows: $\mathcal{A} = 100$, $C = 2$, $p = 10$, $q = 100$, $\mathcal{R} = 20$, $\lambda = 1$ (original parameter values are $\delta = 9 \times 10^{-4}$, $K = 1 \times 10^6$, $a = 0.01$, $H = 1 \times 10^6$, $c = 2 \times 10^6$, $N = 1 \times 10^6$, $r = 0.002$, $\mu = 1 \times 10^{-4}$, $\xi = 0.01$).* (b) *ζ is sufficiently larger than $f'(C)$ ($\zeta = 3.3333$, $f'(C) = 2.0030$). Four equilibrium points exist: two saddle equilibrium points E_1^+ and E_0 and two attracting equilibrium points E_1 and E_2^+. The values used for the parameters are as follows: $\mathcal{A} = 10^3$, $C = 2$, $p = 10$, $q = 10^3$, $\mathcal{R} = 30$, $\lambda = 1$ (original parameter values are $\delta = 9 \times 10^{-4}$, $K = 1 \times 10^6$, $a = 0.1$, $H = 1 \times 10^6$, $c = 2 \times 10^6$, $N = 1 \times 10^6$, $r = 0.003$, $\mu = 1 \times 10^{-4}$, $\xi = 0.1$).*

endemic steady state rather than a disease-free one. So, E_0 is locally unstable, E_1 and E^* are locally stable when they exist, and numerically we see that E_1^+ is unstable and E_2^+ is attracting. We summarize the preceding local stability results with a theorem.

THEOREM 3.4 (local stability). *System* (3.1) *has between two and four equilibria.*

- *When $C < 1$ (equivalently, $c < K$), $E_0 = (1, 0, 0)$ is unstable and a unique endemic equilibrium E^* exists and is locally asymptotically stable.*
- *When $C \geq 1$ (equivalently, $c \geq K$), then $E_0 = (1, 0, 0)$ is unstable and $E_1 = (1, 0, 1)$ is an equilibrium and is locally asymptotically stable. Up to two internal equilibria, $E_{1,2}^+$, can also exist.*

3.5. Global stability of E_1 and E^*. We wish to invoke a theorem of H. Smith in regards to monotone dynamical systems and global stability. Because of the threshold parameter, the Jacobian of (3.1) will have two different forms with $\alpha(B) = 0$ or not. Either way, the Jacobian is of the form

$$J(S, I, B) = \begin{pmatrix} * & + & - \\ + & * & + \\ - & + & * \end{pmatrix},$$

which is sign stable and sign symmetric in the off-diagonal entries. As demonstrated in Figure 7, every closed loop has an even number of edges with + signs and so the system is *monotone*, as defined on page 49 in [5], in Ω with respect to the partial ordering

$$K_m = \{(S, I, B) : S \geq 0, I \leq 0, B \geq 0\}. \tag{5}$$

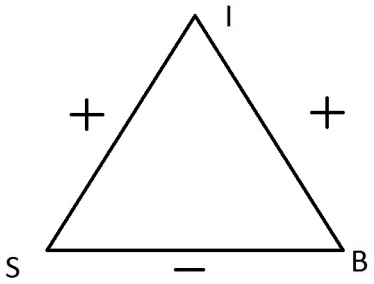

FIG. 7. *The relationship between the three main compartments in the model.*

Our argument is as follows: an application of monotone dynamical system theory states that if system (3.1) has a positive periodic orbit in domain Ω, then there exists an unstable equilibrium in Ω (Proposition 4.3, p. 44, in [5]). When $C \geq 1$ and condition (4) is satisfied ($\zeta < f'(C)$), then there are only E_0 and E_1, neither of which is an interior equilibrium. Hence system (3.1) will not have any periodic orbits in Ω. As (3.1) is competitive, it reduces to a two-dimensional system [5]. Because of the absence of limit cycles and by the Poincaré–Bendixson theory, the local stability of E_1 implies that E_1 is globally asymptotically stable.

Define

$$H_1 = \{(S, I, B) : B \leq C, 0 < S + I \leq 1\},$$
$$H_2 = \{(S, I, B) : C < B < B_{max}, 0 < S + I \leq 1\},$$

and note that $H_1 \subset \Omega, H_2 \subset \Omega$ with $\Omega = H_1 \bigcup H_2$. We will show that when $C \geq 1$ and $\zeta < f'(C)$, after some τ_0 all solutions will stay entirely in H_1 and we can apply our argument about the global asymptotic stability of E_1.

First we require a result from Smith [5] about competitive systems noting first that $\ll_m$ and $\leq_m$ are order relations with respect to K_m defined in (5).

LEMMA 3.5 (Proposition 4.3, p. 44, in [5]). *Let γ be a nontrivial periodic orbit of a competitive system in $D \subset \mathbb{R}^3$ and suppose there exist $p, q \in D$ such that $p \ll_m q$ and $[p, q] = \{y \in D : p \leq_m y \leq_m q\} \subset D$. Then W is an open subset of $\mathbb{R}^3$ consisting of two connected components, one bounded and one unbounded. The bounded component, $W(\gamma)$, is homeomorphic to the open ball in $\mathbb{R}^3$. $W(\gamma) \subset [p, q]$, is positively invariant, and its closure contains an equilibrium.*

Now we require some results about the behavior of solutions of (3.1) with respect to H_1 and H_2.

LEMMA 3.6. *If $C \geq 1$ and $\zeta < f'(C)$, then for all solutions $x(\tau) = (S(\tau), I(\tau), B(\tau))$ of (3.1), if there exists some τ_0 such that $x(\tau_0) \in H_2$, then there exists some $\tau_1 > \tau_0$ such that $x(\tau_1) \in H_1$.*

Proof. Assume $x(\tau) \in H_2$ for some $\tau = \tau_1$. Assume for contradiction that $x(\tau) \in H_2$ for all $\tau > \tau_1$. Then by the monotone dynamical systems (MDS) theory we can reduce this three-dimensional system to a two-dimensional system, as it is competitive, and by the Poincaré–Bendixson theorem we can conclude all omega limit sets are limit cycles or equilibria.

As there is not an interior equilibria in H_2, we can conclude by Lemma 3.5 that there are not any limit cycles in H_2. As there are also no equilibria of any type in H_2, we conclude that $x(\tau)$ exits H_2 at some $\tau_2 > \tau_1$. This contradicts our assumption that $x(\tau) \in H_2$ for all $\tau > \tau_1$ and our Lemma is proven. ∎

LEMMA 3.7. *If $C \geq 1$ and $\zeta < f'(C)$, then for all solutions $x(\tau)$ of (3.1), if there exists s_0, s_1 such that $s_1 > s_0$, where $x(s_0) \in H_2$ and $x(s_1) \in H_1$, then $x(\tau) \in H_1$ for $\tau > s_1$.*

Proof. Suppose there exists s_0 and $s_1, 0 < s_0 < s_1$ such that $x(s_0) \in H_2$ and $x(s_1) \in H_1$. There exists $\tau_0 \in (s_0, s_1)$ such that $B(\tau_0) = C$ and $\dot{B}(\tau_0) < 0$. Suppose there exists $\tau_1 > \tau_0$, where $B(\tau_1) = C, \dot{B}(\tau_1) > 0$, meaning that x(t) is reentering H_2. Choose the first such time τ_1 and note

$$\dot{B}(\tau_1) = \mathcal{R}C(1-C) + qI(\tau_1) > 0,$$
$$\dot{B}(\tau_0) = \mathcal{R}C(1-C) + qI(\tau_0) < 0.$$

This means that $I(\tau_1) > I(\tau_0)$ but $B(\tau) \leq C$ on $\tau_0 < \tau < \tau_1$ and so $\dot{I} = -pI < 0$. This is a contradiction, so there can be no such τ_1 as supposed and the lemma is proven. ∎

Thus no solutions can stay in H_2 as $\tau \to \infty$ and once H_1 is entered from H_2, H_1 is forward invariant. This captures the behavior of all solutions $x(\tau)$.

We can now conclude that E_1 is globally asymptotically stable.

PROPOSITION 3.8 (global stability of E_1). *When $C \geq 1$ and $\zeta < f'(C)$, $E_1 = (1, 0, 1)$ is an equilibrium of (3.1) and it is globally asymptotically stable.*

Proof. When $C \geq 1$ and $\zeta < f'(C)$, by Lemmas 3.6 and 3.7, all solutions eventually exist entirely in H_1 and as there are no interior equilibria (because $\zeta < f'(C)$), by Lemma 3.5 there are no limit cycles in H_1. MDS theory says that (3.1) reduces to a two-dimensional system, and so by the Poincaré–Bendixson theorem all omega-limit sets are limit cycles or equilibria. As there are no limit cycles in H_1 and no interior equilibria, by the local stability of E_1, we conclude that it is globally asymptotically stable. ∎

Now we consider the global stability of E^*. As (3.1) is monotone, it verifies the Poincaré–Bendixson property: every compact omega-limit set without equilibria is a closed orbit. For systems with this property, a criterion on global stability has been developed by Li, and Muldowney [18] and Li and Wang [19]. Note that the *second additive compound* of a 3×3 matrix, $A = [a_{ij}]$, is denoted $A^{[2]}$ and defined

$$A^{[2]} = \begin{bmatrix} a_{11} + a_{22} & a_{23} & -a_{13} \\ a_{32} & a_{11} + a_{33} & a_{12} \\ -a_{31} & a_{21} & a_{22} + a_{33} \end{bmatrix}.$$

LEMMA 3.9 (Theorem 2.5 in [19]). *Let $\dot{x} = F(x) (F \in C^1)$ be a system defined on an open convex subset $G \subset \mathbb{R}^3$ having a compact global attractor in G. Assume that*
1) *the Poincaré–Bendixson property holds;*
2) *there is a unique equilibrium in G which is locally asymptotically stable;*
3) *for each periodic orbit $p(t)$ in G, the linear system*

$$\dot{Y} = \frac{\partial F^{[2]}}{\partial x}(p(t))Y$$

is asymptotically stable.

Then the equilibrium is globally asymptotically stable in G.

In order to apply this result, we have to study the asymptotic stability of the linear equation

$$\dot{Y} = J^{[2]}(p(t))Y, \tag{6}$$

where $p(t)$ is any periodic solution of (3.1) in Ω. Given our definition of J_{E^*}, the second additive compound of J_{E^*} is

$$J^{[2]} = \begin{pmatrix} -f_0(B) - 1 - p & f_0'(B)S & f_0'(B)S \\ q & -f_0(B) - f_1'(B) - 1 & 0 \\ 0 & f_0(B) & -p - f_1'(B) \end{pmatrix},$$

where $f_0(B) = \frac{A(B-C)}{B-C+\lambda}$ and $f_1'(B) = 2\mathcal{R}B - \mathcal{R}$.

Typically verifying the stability of such a system is nontrivial, but for (6) we have a linear, periodic, cooperative, irreducible system with respect to the cone

$$K_1 = \{(S, I, B) : S \geq 0, I \geq 0, B \geq 0\}$$

which suggests we use a comparison result.

LEMMA 3.10 (Proposition 3 in [11]). *Let $\dot{Y} = A_i(t)Y$ for $i = 1, 2$ be two linear, periodic, cooperative, and irreducible systems (with the same period) such that $A_2(t) - A_1(t)$ has nonnegative coefficients. If $\dot{Y} = A_2(t)Y$ is asymptotically stable, then $\dot{Y} = A_1(t)Y$ is too.*

For our case, obviously$A_1 = J^{[2]}(p(t))$ and for A_2 we choose a constant matrix whose entries bound those of A_1 independently of the periodic orbit and denote the matrix $\bar{J}$ where

$$\bar{J} = \begin{pmatrix} -1 - p - f_0(1) & f_0'(1) & f_0'(1) \\ q & -f_0(1) - f_1'(1) - 1 & 0 \\ 0 & f_0(B_{max}) & -p - f_1'(1) \end{pmatrix}.$$

The characteristic equation, $P(\gamma)$, of $\bar{J}$ is

$$P(\gamma) = [\gamma+1+p+f_0(1)][\gamma+1+f_0(1)+f_1'(1)][\gamma+p+f_1'(1)] - qf_0'(1)[\gamma+p+f_1'(1)+f_0(B_{max})].$$

Expanding this out we can write

$$P(\gamma) = a_3\gamma^2 + a_2\gamma^2 + a_1\gamma + a_0$$

with coefficients

$$\begin{aligned} a_3 &= 1, \\ a_2 &= 2(1 + p + f_0(1) + f_1'(1)), \\ a_1 &= [2 + 2f_0(1) + p + f_1'(1)](p + f_1'(1)) + [1 + p + f_0(1)](1 + f_0(1) + f_1'(1)) - qf_0'(1), \\ a_0 &= [1 + p + f_0(1)](1 + f_0(1) + f_1'(1))[p + f_1'(1)] - qf_0'(1)[p + f_1' + f_0(B_{max})]. \end{aligned}$$

To use the Routh–Hurwitz conditions, we require that $a_i > 0$ and that $a_1a_2 > a_3a_0$. First, we consider the positivity of the coefficients. Only the positivity of a_1 and a_0 require checking:

$$\begin{aligned} a_0 &> p + pf_1'(1) + p^2f_1'(1) + pf_1'(1) + pf_1'(1)f_1'(1) + f_1'(1)f_1'(1) \\ &\quad - qA\lambda^{-1}(p + f_1'(1) + A)) \\ &= (p+1)^2f_1'(1) + p^2 + p + pR^2 + R^2 - qA\lambda^{-1}(p + f_1'(1) + A)). \end{aligned}$$

Noting that $f_1'(1) = \mathcal{R} = \frac{r}{\mu}$ it is reasonable to assume that $\mathcal{R} > 1$ as μ is the human birth/date rate and will be very small. Also r, the maximum bacterial growth rate, is often greater than 1. Finally, by definition $p > 1$, thus

$$\begin{aligned} a_0 &> (p+1)^2\mathcal{R} + p^2 + p + p\mathcal{R}^2 + \mathcal{R}^2 - qA\lambda^{-1}(p + \mathcal{R} + A)) \\ &> (p+1)^2\mathcal{R} + (p+1)^2 - qA\lambda^{-1}(p + A) - qA\lambda^{-1}\mathcal{R}. \end{aligned}$$

Suppose the parameters p, q, A, and λ are such that

$$(p+1)^2 > qA\lambda^{-1}(p+A). \tag{7}$$

Then $a_0 > 0$. The positivity of a_1 follows similarly,

$$a_1 > (2+p)p + (1+p) - qA\lambda^{-1} > (1+p)^2 - qA\lambda^{-1},$$

and if the parameters satisfy (7), then $a_1 > 0$ too. Now we can consider $\triangle = a_1a_2 - a_3a_0$,

$$\begin{aligned}
\triangle &= 2(1+p+f_0(1)+f_1'(1))\{(1+f_0(1)+p)(p+f_1'(1)) \\
&\quad + [1+p+f_0(1)][1+f_0(1)+f_1'(1)]\} + [1+p+f_0(1)](1+f_0(1)+f_1'(1))[p+f_1'(1)] \\
&\quad + 2f_1'(1)[1+f_0(1)+f_1'(1)](p+f_1'(1)) + qf_0'(1)[-2-p-2f_0(1)-f_1'(1)+f_0(B_{max})], \\
&> 2(1+p+f_0(1)+f_1'(1))(1+p)p + (1+p) - qf_0'(1)[2+2p+f_0(1)+2f_1'(1)] \\
&= 2(1+p+f_0(1)+f_1'(1))\Big[(1+p)^2 - qf_0'(1)\Big].
\end{aligned}$$

Note that $(1+p)^2 - qf_0'(1) > (1+p)^2 - qA\lambda^{-1}$ and if the parameters satisfy (7), we have that $a_2a_1 > a_3a_0$. Lastly, considering H_1 and H_2 as before, note that if $C < 1$ then $\dot{B}(B = C) = \mathcal{R}C(1-C) + qI > 0$, so eventually all trajectories exist entirely in H_2. In particular, any attracting limit cycles are contained in H_2. We restate the previous results in a proposition.

PROPOSITION 3.11 (behavior of limit cycles and global stability of E^*). *When $C < 1$, E^* is an equilibrium of* (3.1). *Any limit cycle, if it exists, should be entirely in H_2, and if $(p+1)^2 > qA\lambda^{-1}(p+A)$, then E^* is globally asymptotically stable.*

Recalling that $C = c/K$, we can summarize our results about the equilibria in this section with the following theorem.

THEOREM 3.12 (global stability). *System* (3.1) *always has at least two equilibria.*

- *If $C < 1$ (equivalently, $c < K$), the equilibria are $E_0 = (1,0,0)$ which is unstable and $E^* = (S^*, I^*, B^*)$ which is locally asymptotically stable. Furthermore, if $(p+1)^2 > qA\lambda^{-1}(p+A)$, then E^* is globally asymptotically stable.*
- *If $C \geq 1$ (equivalently, $c \geq K$), the equilibria are $E_0 = (1,0,0)$ which is unstable, $E_1 = (1,0,1)$ which is locally asymptotically stable, and up to two internal equilibria $E_{1,2}^+$.*
  Further, if $\zeta < f'(C)$, only E_0 and E_1 exist, and E_1 is globally asymptotically stable.

Note that if the MID is greater than K and ζ is low enough to satisfy condition (4), the disease-free equilibrium E_1 is globally asymptotically stable. As nondimensional ζ and the shedding parameter ξ are proportional, this means that with a nonzero but sufficiently small shedding rate, the disease-free equilibrium is inevitable. This is in contrast to the case where the MID is less than the carrying capacity of bacteria, and the bacteria exist at levels which naturally cause new infections. In this case, if other parameters agree, the endemic steady state E^* is globally asymptotically stable for any nonzero shedding rate ξ. Thus if efforts are taken to decrease K and ξ in conjunction, a disease-free globally stable steady state can be attained with a shedding rate that could otherwise lead to an endemic steady state.

Remark 3.13 (biological interpretation of the sufficient condition for globally asymptotic stability of E^*). In terms of the original parameters, $(p+1)^2 > qA\lambda^{-1}(p+A)$ could be written as $N < \frac{\mu H(\delta+2\mu)^2}{\xi a(\mu+\delta+a)} := N_c$. N_c is a critical population level below which the endemic equilibrium E^* is globally attracting. If we

consider towns with similar population densities and sanitation infrastructures, and with their pathogen carrying capacity in the reservoir over their rescaled MID, a small population size is associated with a small town, which results in a strong connection between individuals and pathogens. Hence, a small population size leads to the robust and persistent disease prevalence in the case that the pathogen carrying capacity is greater than the MID. Note that the given inequality is a sufficient but not necessary condition, thus a large city ($N \geq N_c$) with some restrictions may also lead to the globally attracting E^*. With the limitation of existing mathematical techniques, the sufficient condition is the best condition we can obtain for the global stability of the internal equilibrium. Using the reasonable parameter values, N_c can reach up to 2.5439×10^6.

4. Numerical simulations. Stability was discussed nondimensionally previously but numerical examples are presented in the following diagrams in dimensional parameters. In Figure 8, we see that if $c \geq K$ ($\mathbf{C} > 1$) with a small ξ value, meaning the MID is larger than the carrying capacity, then there is no endemic equilibrium. Thus the system moves towards the disease-free steady state. Intuitively, this means that it takes more than the "natural level" of bacterial density in the water supply to make anyone sick and shedding is low, so no one becomes sick.

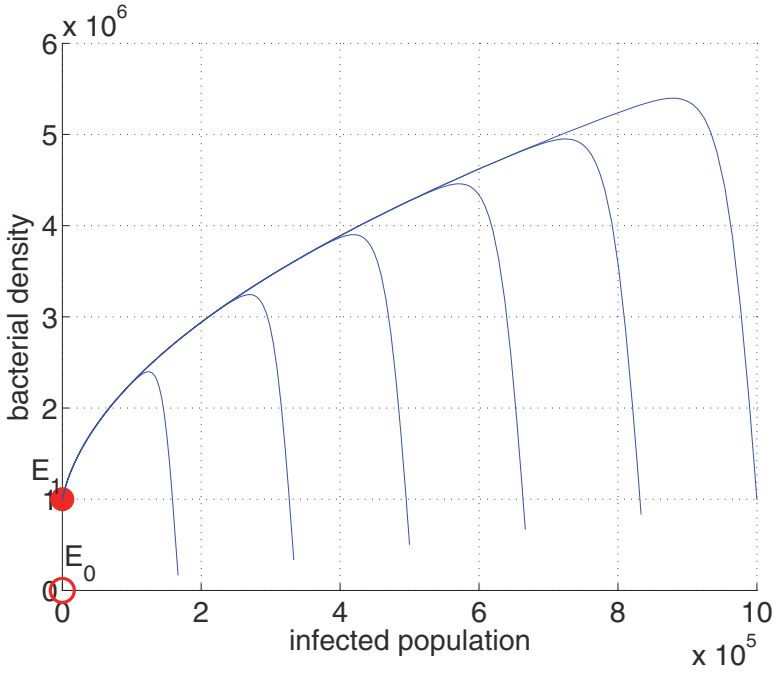

FIG. 8. *Phase portrait for $c > K$, showing trajectories with different initial conditions converging to the disease-free steady state E_1. Parameter values used are $\delta = 0.1$, $K = 1 \times 10^6$, $a = 0.1$, $H = 1 \times 10^8$, $c = 2 \times 10^6$, $N = 1 \times 10^6$, $r = 0.3704$, $\mu = 5 \times 10^{-5}$, $\xi = 10$.*

Figure 9 demonstrates that when the MID is less than the carrying capacity, $c < K$, then the internal endemic steady state is attracting. In it, a wide range of initial conditions all follow a similar path towards the endemic steady state after each trajectory first experiences an outbreak. This means that if the MID is small enough that a normal bacterial density can make any individual sick, then the disease will

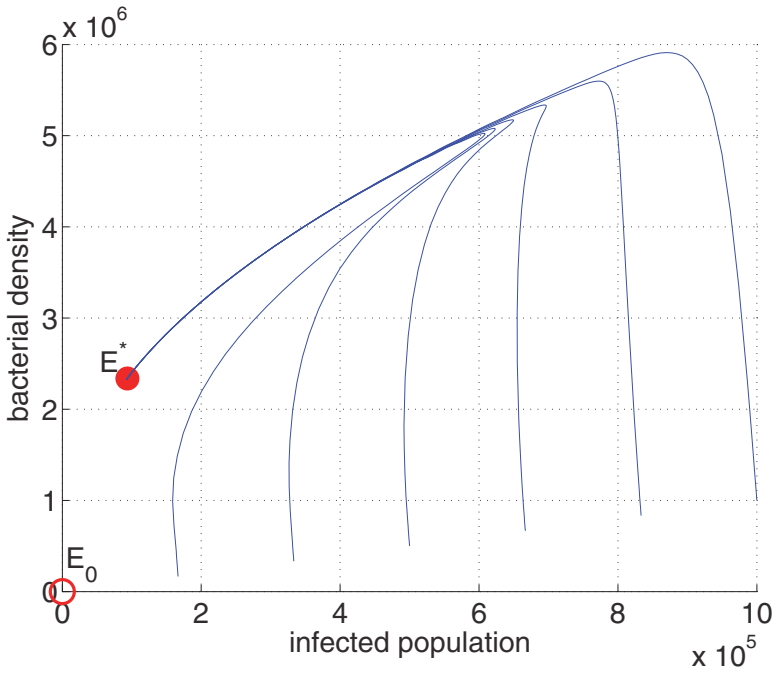

FIG. 9. *Phase portrait for $c < K$, showing many different trajectories approaching the endemic steady state, marked with a solid circle. Parameter values used are $\delta = 9 \times 10^{-4}$, $K = 1 \times 10^6$, $a = 0.1$, $H = 1 \times 10^8$, $c = 8 \times 10^5$, $N = 1 \times 10^6$, $r = 0.003$, $\mu = 5 \times 10^{-4}$, $\xi = 0.1$.*

persist in the community if only at a low level. As mentioned, a strong epidemic always occurs with a high outbreak peak.

5. Local sensitivity analysis. In this section, we compute and analyze the normalized forward sensitivity indices (S.I.) of different quantities to the parameters of the system by computing

$$S.I. = \frac{\partial x^*}{\partial p}\frac{p}{x^*}, \tag{8}$$

where x^* is the quantity being considered and p is some parameter which x^* depends upon. Sensitivity indices can be positive or negative which indicates the nature of the relationship, and it is the magnitude that ranks the strength of the relationship as compared to the other parameters. Since we don't have an explicit formula for the quantities we are interested in (outbreak peak, outbreak peak time, and the endemic steady state), we estimate $\frac{\partial x^*}{\partial p}$ using the central difference approximation:

$$\frac{\partial x^*}{\partial p} = \frac{x^*(p + \Delta p) - x^*(p - \Delta p)}{2\Delta p} + \mathcal{O}(\Delta p^2).$$

We choose $\Delta p = 1\%$ of p. Plugging all these in (8) we get

$$S.I = \frac{x^*(1.01p) - x^*(0.99p)}{0.02x^*}.$$

5.1. Sensitivity of the outbreak peak. The sensitivity indices of the amplitude of the outbreak peak show how the first epidemic depends on the parameters as seen in Table 3. This table has three columns because there is a noticeable difference in the sensitivity indices when the bacteria started out above or below the carrying capacity.

TABLE 3
The sensitivity of the magnitude of the peak outbreak to the parameters. Two columns for the initial density of the bacteria below or above their carrying capacity K.

Parameter	Sensitivity B(0) < K	Sensitivity B(0) > K	
δ	−1.2024	−0.5296	Recovery rate
K	1.8773	1.1334	Bacterial carrying capacity
a	1.1980	0.9822	Contact rate
H	−1.1905	−0.9623	Half-saturation constant
c	−0.9324	−0.4196	MID
r	−0.2305	−0.5267	Logistic bacterial growth
μ	−5.5e-004	−2.5830 e-004	Human birth/death
ξ	0.2352	0.0636	Shedding rate

The carrying capacity K has the strongest relationship to the magnitude of the outbreak peak. The positive value tells us that a higher carrying capacity would lead to a more severe epidemic. In contrast to the shedding rate ξ which has among the lowest of sensitivity indices, K would thus be an important parameter to control in order to reduce the harm of an outbreak.

A negative relationship between r and the peak magnitude might seem counterintuitive, but the per capita growth rate of bacteria at any given time is $r\left(1-\frac{B}{K}\right)$ and during the peak the bacteria exist over their natural carrying capacity, so the growth rate would be negative and thus there is a negative relationship between r and the peak amplitude.

The sensitivity index with respect to the human birth/death rate μ is very low in comparison to all the others. This makes sense, because the initial peak of an epidemic occurs relatively quickly after the introduction of sick people or introduction of high levels of bacteria and the birth and death of new susceptibles would not be on the same time scale.

A negative relationship between the MID c and peak amplitude is consistent with our understanding of the disease dynamics, because a larger MID means it would take a higher bacterial density to cause any infections at all. Thus a higher MID would mean less infections and a smaller outbreak peak.

The recovery rate δ has a strong negative relationship to the peak outbreak level as a higher δ leads to few infectives by definition.

5.2. Sensitivity of the outbreak peak time. Once again we see from Table 4 that the carrying capacity K has a large influence on the dynamics of the system. It has one of the largest sensitivity indices, being many times greater than that of the shedding rate ξ. This suggests that K is a more important quantity to control to prevent outbreaks. The positive relationship means a smaller carrying capacity would lead to a quicker outbreak as well as a smaller one as we saw in the last section. Noticeable is the lack of effect of μ, as with the amplitude of the peak. It has such a negligible effect for the same reasons as outlined previously.

The relationship between contact rate a and the time of the maximum outbreak is a negative relationship, because a higher contact rate causes more new infections and so the timing of the maximum would be attained earlier than otherwise.

TABLE 4
The sensitivity of the time of the outbreak maximum to the parameters.

Parameter	Sensitivity B(0) < K	Sensitivity B(0) > K	
δ	0.0772	−6.7542	Recovery rate
K	0.4392	4.8433	Bacterial carrying capacity
a	−0.2177	−0.3361	Contact rate
H	0.2159	0.3264	Half-saturation constant
c	0.9319	0.0928	MID
r	−0.6327	3.9216	Logistic bacterial growth
μ	3.5491e-005	4.3194e-005	Human birth/death
ξ	−0.2269	−0.1425	Shedding rate

The recovery rate δ is interesting because its effect changes sign as well as magnitude considerably with different values of $B(0)$ in relation to carrying capacity. When $B(0) > K$ the effect of δ is greatest and negative. A higher value of δ would mean individuals would be infected, and thus infectious, for less time, so the outbreak should not be as severe and would occur earlier than otherwise. As the magnitude of δ is so small when it is positive, the positive relationship does not yield insight into the relationship of outbreak time and recovery rate.

The per capita growth rate is $r\left(1-\frac{B}{K}\right)$ and so when $B > K$ this growth rate is negative. If $B(0) < K$ then the growth rate will be positive in the beginning of the outbreak, so a larger r would mean a higher growth rate, and thus the epidemic would peak earlier. This is supported by the negative relationship with r and peak time when $B(0) < K$. If however $B(0) > K$, the per capita growth rate will be negative from the start, and as B will remain above K for all time, the growth rate will always be negative. So a larger r value would mean slower growth, and the epidemic wave would take longer to reach a maximum. This is supported by the strong positive relationship of r and peak time when $B(0) > K$ as can be seen in Table 4.

TABLE 5
The sensitivity of the components of the endemic equilibrium.

Parameter	Sensitivity of S^*	Sensitivity of I^*	Sensitivity of B^*	
δ	0.0321	−0.9453	−0.0780	Recovery rate
K	−1.9877	−0.1036	1.0666	Bacterial carrying capacity
a	−1.0314	−0.0611	0.0402	Contact rate
H	1.0260	0.0606	−0.0399	Half-saturation constant
c	0.9932	0.0225	0.0014	MID
r	0.0323	−0.0329	0.0474	Logistic bacterial growth
μ	0.8472	0.8177	0.0811	Human birth/death
ξ	−0.0323	0.0123	−0.0179	Shedding rate

5.3. Sensitivity of the endemic steady state. We can look at the sensitivity of one of the interior equilibria E^* with respect to the parameters when E^* exists. In Table 5 we only look at $B(0) < K$ as the other case has similar sensitivity results, and we assume the other endemic steady states would yield similar results.

The final size of the susceptible population is most sensitive to the carrying capacity K and contact rate a, with a negative relationship in both cases. This is because a higher contact rate causes more infections and a higher carrying capacity causes more

bacteria which indirectly leads to more infections. A higher shedding rate would cause more infections which is confirmed with the negative relationship between S^* and ξ. But S^* is many times less sensitive to ξ than to K which again points to K as the more important parameter to focus on in disease control. The MID c is nearly as sensitive as the contact rate, but has a positive relationship as a higher MID would lead to fewer infections and a higher S^*. There is a weak relationship with δ but as our model does not allow for reinfection, this accounts for the small magnitude of the sensitivity.

The endemic level of infective individuals is most sensitive to the recovery rate δ and the birth/death rate μ. The strong negative relationship with δ is because recovery is the main way that infectives leave the infected component of our model. The relationship with μ is complicated in that the birth rate and death rate are the same in our model. So a larger μ means more deaths and thus more infectives leaving the infected component, but also more newly born susceptibles to possibly enter the infected class. The positive relationship means that the positive effect of births is more important to I^* than the negative effect of deaths. The shedding rate ξ has a weak relationship with I^* but the positive relationship is as expected because a larger ξ leads to more infectives and a higher I^* value.

The endemic level of the bacterial population is most sensitive to the bacterial carrying capacity K and has a positive relationship to it as expected. A higher K means more bacteria and as $B^* > K$ (equivalent to $B^* > 1$ in nondimensional form) the relationship is positive. The shedding rate has a small sensitivity which suggests that the logistic part of $\frac{dB}{dt}$ is more important to the endemic level of B^*. As such the relationship with the MID is also minimal. The strong relationship with K and weak one with ξ also again suggests the importance of K instead of ξ as a control measure. This could mean, for example, that monitoring the bacterial levels in water reservoirs is more important than simply controlling or restricting access to the water supply to avoid contamination.

6. Discussion. Cholera has the potential to quickly spread over large areas and can cause many deaths. Thus a full understanding of the dynamics is essential to effectively respond to outbreaks. With the continuing outbreaks there is the opportunity for mathematical modeling to help decipher these dynamics and provide suggestions for governments and health care bodies in effective intervention. An estimate for the basic reproductive number in regions affected by cholera would give important information for controlling future outbreaks and for creating surveillance programs. The potential for amplification in environmental reservoirs and the indirect transmission of the disease make this a nontrivial task. Here we have shown that with $\mathbf{C} = c/K \geq 1$, the disease-free equilibrium can be globally asymptotically stable. However as bacteria are existing at a nonzero level, if environmental factors change and alter the carrying capacity enough to make $\mathbf{C} < 1$, then there can be outbreaks. If other parameters are in agreement, an endemic equilibrium is globally asymptotically stable. This change to carrying capacity could be seasonally caused as with different amounts of rain in areas like Bangladesh, or it could be a more permanent change due to natural disasters as in Haiti.

An important thing to note about the relationship between c and K is that if $c < K$, i.e., the MID is less than the carrying capacity, then the unique endemic equilibrium can be globally stable. It is globally stable for any nonzero value of the shedding parameter ξ. If however, the MID is greater than the natural carrying capacity, if ξ is low enough, causing the nondimensional ζ to be sufficiently small, then

the disease-free equilibrium becomes globally stable. This highlights the importance of being aware of the value of the natural carrying capacity, because decreasing the shedding rate can eliminate the possibility of an endemic steady state, if the MID is larger than the carrying capacity. If the MID was less than the carrying capacity, the unique endemic steady state could be globally asymptotically stable for the same shedding rate. So ideally, efforts need to be taken to reduce both shedding, and in conjunction with this, the bacterial levels in the reservoir.

Our sensitivity analysis suggests that control measures influencing the carrying capacity K will be more effective in minimizing the epidemic than those concentrating on influencing the shedding rate. While improving the sanitation infrastructure of an area is the obvious step to take to control outbreaks, monitoring and controlling the bacterial levels in the water itself is more important. Improving the infrastructure would surely help control the bacterial levels in the water by decreasing the amount of human contamination, but *V.cholerae* exist independently of humans and so other factors that influence the natural levels of bacteria in the water need to be considered as well in intervention strategies. As mentioned above, controlling both parameters is important and likely to be the most effective, but the carrying capacity K is the more influential of the two on its own.

Our analysis accounts for all the situations experienced all over the world. Should the average health and immune system capabilities of the population be sufficient to tolerate bacterially contaminated water, and the shedding rate be sufficiently small, the human and bacteria populations will exist independently of each other. This case reflects both interepidemic periods where cholera outbreaks are common, and also the situation in regions where cholera outbreaks are not experienced. Should, however, the carrying capacity be sufficiently high (enough to overwhelm the average immune response of the human population), an endemic steady state will exist that can be globally stable. If this situation is only temporary, the iSIR model can thus account for isolated outbreaks of cholera, and if it persists, the model is suitable for regions where cholera cases are constant occurrences.

The original paper of the iSIR model [25] provided some preliminary mathematical results. This analysis adds on to that work, and demonstrates the local stability for most equilibria analytically. In addition, we present the results of dissipativity and determine conditions for global stability.

Further steps to take with this model would be to refine the condition on the global stability of the endemic equilibrium. The condition imposed might not be required, and a biological explanation is in order. Also, a seasonal carrying capacity could be included to simulate the cycles of cholera which occur in regions like Bangladesh. Further altering the model to include bacteriophage is another possibility, with the idea being that the cycles observed in the human population are caused by cycles in the microscale of bacteria and bacteriophage as has been suggested by Faruque et al. [28] and others.

REFERENCES

[1] B. S. Fields, R. F. Benson, and R. F. Besser, *Legionella and Legionnaires' disease:* 25 *years of investigation*, Clinical Microbiol. Rev., 15 (2002), pp. 506–526.

[2] C. T. Codeço, *Endemic and epidemic dynamics of cholera: The role of the aquatic reservoir*, BMC Infect. Diseases 1 (2001), 1.

[3] D. M. Hartley, J. G. Morris, and D. L. Jr., Smith, *Hyperinfectivity: A critical element in the ability of V. cholerae to cause epidemics?*, PLoS Med 3 (2006), e7.

[4] H. L. DuPoint, C. L. Chappell, C. R. Sterling, P. C. Okhuysen, J. B. Rose, and W. Jakubowski, *The infectivity of* crytosporidium parvum *in healthy volunteers*, New England J. Med., 332 (1995), pp. 855–859.
[5] H. Smith, *Monotone Dynamical Systems: An Introduction to the Theory of Competitive and Cooperative Systems*, Math. Surveys Monogr. 41, AMS, Providence, RI, 1995.
[6] J. B. Rose, *Environmental ecology of* crptosporidium *and public health implications*, Annu. Rev. Public Health, 18 (1997), pp. 135–161.
[7] J. B. Kaper, J. G. Morris, Jr., and M. M. Levine, *Cholera* Clinincal Microbiol. Rev., 8 (1995), pp. 48–86.
[8] J. H. Tien and D. J. D. Earn, *Multiple Transmission Pathways and Disease Dynamics in a Waterborne Pathogen Mode*, Bull. Math. Biol., 72 (2010), pp. 1506–1533.
[9] J. P. Tian and J. Wang, *Global stability for cholera epidemic models*, Math. Biosci., 232 (2011), pp. 31–41.
[10] K. M. Murphy, P. Travers, and M. Walport, *Janeway's Immunobiology*, 7th ed., Garland Science, New York, 2007.
[11] L. A. Sanchez, *Dynamics of the modified Michaelis-Menten system*, J. Math. Anal. Appl., 317 (2006), pp. 71–79.
[12] L. Chitsulo, D. Engles, A. Montresor, and L. Savioli, *The global status of schistosomiasis and its control*, Acta Trop., 77 (2000), pp. 41–51.
[13] M. A. Jensen, S. M. Faruque, J. J. Mekalanos, and M. A. Levin, *Modeling the role of bacteriophage in the control of cholera outbreaks*, Proc. Natl. Acad. Sci. USA, 103 (2006), pp. 4652–4657.
[14] M. K. Estes, E. L. Palmer, and J. F. Obijeski, *Rotavirus: A review*, Current Top. Microbiol. Immunol., 105 (1983), pp. 123–184.
[15] M. M. Levine, R. E. Black, M. L. Clements, D. R. Nalin, L. Cisneros, and R. A. Finkelstein, *Volunteer studies in development of vaccines against cholera and enterotoxigenic* escherichia coli*: A review, in Acute Enteric Infections in Children. New Prospects for Treatment and Prevention*, T. Holme, J. Holmgren, M. H. Merson, and R. Molby, eds., Elsevier/North-Holland Biomedical Press, Amsterdam, 1981, pp. 443–459.
[16] M. S. Wolfe, *Giardiasis*, Clinical Microbiol., 5 (1992), pp. 93–100.
[17] M. W. LeChevallier, W. D. Norton, and R. G. Lee, *A contribution to the mathematical theory of epidemics*, R. Soc. Lond. Proc. Ser. A Math. Phys. Eng. Sci., 115 (1995), pp. 48–86.
[18] M. Y. Li and J. S. Muldowney, *Global stability for the SEIR model in epidemiology*, Math. Biosci., 125 (1995), pp. 155–164.
[19] M. Y. Li and L. Wang, *Global stability in some SEIR epidemic models*, in Mathematical Approaches for Emerging and Reemerging Infectious Diseases: Models, Methods, and Theory, IMA Vol. Math. Appl., 126 (2000), pp. 295–311.
[20] P. O. White and F. J. Fenner, *Medical Virology*, 4th ed. Academic, San Diego, 1994.
[21] P. R. Brayton, M. L. Tamplin, A. Huq, and R. R. Colwell, *Enumeration of* vibrio cholerae O1 *in Bangladesh waters by fluorecescent-antibody direct viable count*, Appl. Environ. Microbiol., 53 (1987) pp. 2862–2865.
[22] R. A. Cash, R. A. Music, J. P. Libonati, M. J. Snyder, R. P. Wenzel, and R. B. Hornick, *Response of man to infection with* Vibrio cholerae *I. Clinical., serologic, and bacteriologic responses to a known inoculum*, J. Infect. Diseases, 129 (1974), pp. 45–52.
[23] R. B. Hornick, S. I. Music, and R. Wenzel, *The Broad Street pump revisited: Response of volunteers to ingested cholera Vibrio*, Bull. New York Acad. Med., 47 (1971), pp. 1181–1191.
[24] R. C. Rendtorff, *The experimental transmission of human intestinal protozoan parasites:* Giardia lamblia cyst *given in capsules*, Amer. J. Hyg., 59 (1954), pp. 209–220.
[25] R. I. Joh, H. Wang, H. Weiss, and J. S. Weitz, *Dynamics of indirectly transmitted infectious diseases with immunological threshold*, Bull Math Biol., 71 (2009), pp. 845–862.
[26] R. L. Ward, D. L. Bernstein, E. C. Young, J. R. Sherwood, D. R. Knowlton, and G. M. Shiff, *Human rotavirus studies in volunteers: Determination of infectious dose and serological respons to infection*, Infectious Diseases, 154 (1986), pp. 871–880.
[27] R. R Colwell, P. Brayton, D. Herrington, B. Tall, A. Huq, and M. M Levine, *Viable but non-culturable* Vibrio cholerae *O*1 *revert to a cultivable state in the human intestine*, World J. Microbiol. Biotech., 12 (1996), pp. 28–31.
[28] S. M. Faruque, I. B. Naser, M. J Islam, A. S. G. Faruque, A. N. Ghosh, G. B. Nair, D. A. Sack, and J. J. Mekalanos, *Seasonal epidemics of cholera inversely correlate with the prevalence of environmental cholera phages*, Proc. Natl. Acad. Sci. USA., 102 (2005), pp. 1702–1707.

[29] S. R. Zaki, P. W. Greer, L. M. Coffield, C. S. Goldsmith, K. B. Nolte, K. Foucar, R. M. Feddersen, R. E. Zumwalt, G. L. Miller, A. S. Khan, P. E. Rollin, T. G. Ksiazek, S. T. Nichol, B. W. J. Mahy, and C. J. Peters, *Hantavirus pulmonary syndrome-pathogenesis of an emerging infectious disease*, Amer. J. Pathol., 146 (1995), pp. 552–579.

[30] V. Capasso and S. L. Paveri-Fontana, *A mathematical model for the* 1973 *cholera epidemic in the European Mediterranean region*, Rev. Epidemiol. Sante Publique, 27 (1979), pp. 121–132.

[31] W. O. Kermack and A. G. McKendrick, A *contribution to mathematical theory of epidemics*, R. Soc. Lond Proc. Ser. A. Math. Phys. Eng. Sci., 115, 1927, pp. 700–721.

[32] Z. Mukandavire, S. Liao, J. Wang, H. Gaff, D. L. Smith, and J. G. Morris, Jr., *Estimating the reproductive numbers for the* 2008–2009 *cholera outbreaks in Zimbabwe*, Proc. Natl. Acad. Sci. USA., 108 (2011), pp. 8767–8772.